Quasi-Classical Trajectory Calculations Analyzing the Dynamics of the C−H Stretch Mode Excitation in the H + CHD_3 Reaction

J. Espinosa-García[†]

Departamento de Química Física, Universidad de Extremadura, 06071 Badajoz, Spain

Received: April 2, 2007; In Final Form: May 11, 2007

A state-to-state dynamics study was performed at a collision energy of 1.53 eV to analyze the effect of the C−H stretch mode excitation on the dynamics of the gas-phase H + CHD_3 reaction, which can evolve along two channels, H-abstraction, CD_3 + H_2, and D-abstraction, CHD_2 + HD. Quasi-classical trajectory calculations were performed on an analytical potential energy surface constructed previously by our group. First, strong coupling between different vibrational modes in the entry channel was observed; i.e., the reaction is nonadiabatic. Second, we found that the C−H stretch mode excitation has little influence on the product rotational distributions for both channels, and on the vibrational distribution for the CD_3 + H_2 channel. However, it has significant influence on the product vibrational distribution for the CHD_2 + HD channel, where the C−H stretch excitation is maintained in the products, i.e., the reaction shows mode selectivity, reproducing the experimental evidence. Third, the C−H stretch excitation by one quantum increases the reactivity of the vibrational ground-state, in agreement with experiment. Fourth, the state-to-state angular distributions of the CD_3 and CHD_2 products are reported, finding that for the reactant ground-state the products are practically sideways, whereas the C−H excitation yields a more forward scattering.

1. Introduction

The dynamics of vibrationally excited polyatomic reactions has focused the attention of a growing number of researchers in recent years due to the development of new experimental techniques and theoretical methods. In a series of pioneering studies, Zare and co-workers[1−3] and Crim and co-workers[4−6] analyzed the effects of both reactant stretching and bending excitations on the dynamics of polyatomic systems.

These dynamics studies on polyatomic reactions present a challenge both theoretically and experimentally, and the reaction of hydrogen with methane and its isotopic analogues is the prototypical gas-phase reaction. Very recently, Zare and co-workers[7] carried out experimental studies on the effect of the C−H stretch excitation on the H + CHD_3 reaction, which can evolve along two channels, H- and D-abstraction,

$$\begin{aligned} H + CHD_3 &\rightarrow CD_3 + H_2 \\ &\rightarrow CHD_2 + HD \end{aligned}$$

Those authors reported first that due to experimental difficulties the ground-state reaction shows no clear preference for the H- or D-abstraction channel, second, that the C−H excitation enhances the reactivity for both channels, and third, that the C−H excitation is maintained in the CHD_2 product, which suggests mode selectivity. Theoretically, Xie and Bowman[8] reported recently quasi-classical trajectory (QCT) calculations for the title reaction on an ab initio CH_5 potential energy surface (ZBB3) from the same group.[9,10] The ZBB3 PES is based on accurate fitting of roughly 20 000 CCSD(T)/aug-cc-pVTZ electronic energies. They calculated cross-sections and angular and internal energy distributions for the CHD_3 vibrational ground-state and C−H stretch mode excitation and made direct comparisons with experiment.

In 2002, we developed an analytical potential energy surface (PES-2002) to describe the H + CH_4 reaction and its isotope analogues.[11] Kinetically, it reproduces the behavior of the experimental thermal rate constants and kinetic isotope effects. Dynamically, quasi-classical trajectory (QCT) calculations were performed to analyze the state-to-state dynamics of the vibrational ground-state H + CD_4 reaction,[12,13] and to analyze the role played by the C−H asymmetric stretch mode excitation of methane in the H + CH_4 reaction.[14] The reasonable agreement found with this wide variety of experimental kinetics and dynamics measurements (always qualitative, and sometimes quantitative) lends confidence to the PES-2002 polyatomic surface.

To shed more light on the role of the C−H stretch excitation, in this paper we perform an exhaustive state-to-state dynamics study of the H + CHD_3 reaction using QCT calculations on the PES-2002 surface. The article is structured as follows: In Section 2, we briefly outline the potential energy surface and the computational details. The QCT dynamics results are presented in Section 3 and compared with experimental and previous theoretical results. Finally, Section 4 presents the conclusions.

2. Potential Energy Surface and Computational Details

In 2002, our group constructed a new PES for the gas-phase H + CH_4 → H_2 + CH_3 polyatomic reaction and its isotope analogues,[11] which is symmetric with respect to the permutation of the methane hydrogen atoms, a feature especially interesting for dynamics calculations. The functional form was developed in that work and, therefore, will not be repeated here. Basically, it consists of four LEP-type stretching terms (str), augmented by out-of-plane (op) bending and valence (val) bending terms.

[†] To whom correspondence should be addressed. E-mail: joaquin@unex.es.

10.1021/jp072562b CCC: $37.00
Published on Web 06/14/2007

Note that in this PES, the vibrational frequencies are harmonic. In the calibration process we fitted 35 parameters of the analytical PES to reproduce the variation of the experimental thermal forward rate constants with temperature. The calibration process was widely explained in the original paper,[11] and basically, it consists of three iterative steps. In the first step, we change some parameters of the PES so that the geometries, energy, and vibrational frequencies of the reactants and products agree reasonably with the available experimental data. In a second step, we refit some parameters to reproduce the characteristics of the ab initio calculated saddle point (geometry, vibrational frequencies, and barrier height). Finally, as the third step of the calibration, we refit some parameters to calibrate the PES against experimental forward rate constants. Therefore, because experimental and theoretical ab initio information is used in the calibration process, the present PES is semiempirical.

Because of the great quantity of experimental information available for this reaction, this PES-2002 was subjected to a great variety of tests, in both kinetics and dynamics. The forward and reverse thermal rate constants calculated using variational transition-state theory (VTST) with semiclassical transmission coefficients agree with experimental measurements, reproducing the curvature of the Arrhenius plot, and the experimental activation energy. Second, the experimental kinetic isotope effects (KIEs) are reproduced. Note that these KIEs are a very sensitive test of features of the new surface, such as barrier height and width, zero-point energy, and tunneling effects. Moreover, recently Zhao et al.[15] applied the quantum instanton approximation for thermal rate constants to this reaction using the PES-2002. They find that the quantum instanton rates reproduce the available experimental data over the wide temperature range 200−2000 K and concluded that this result lends support to the accuracy of the present potential surface.

Dynamically, an extensive study employing quasi-classical trajectory (QCT) calculations was also performed on this surface, including both ground-state and the asymmetric vibrationally excited C−H stretching methane. First, whereas QCT calculations fail to reproduce the experimental CD_3 product angular distribution in the H + CD_4 → CD_3 + HD ground-state reaction,[11] this angular distribution is reproduced when reduced dimensionality quantum-scattering (QM) calculations, using the so-called rotating line umbrella (RLU) model, are performed. Second, excitation of the C−H asymmetric stretch mode in methane enhances the forward rate constants by a factor of 2[12] compared to the experimental value 3.0 ± 1.5.[3] In sum, this reasonable agreement with a great variety of kinetics and dynamics results lends confidence in this PES-2002 polyatomic surface, although there are some differences that may be due to the PES (especially the barrier height) but also to the known limitations of the QCT method (especially the binning procedure).

Although the kinetic study is not the main focus of the present study, for clarity of the reader, some kinetics parameters are included for the present reaction, H + CHD_3. The forward thermal rate constants were calculated using also variational transition-state-theory (VTST) with semiclassical transmission coefficients. The values at 298 K, in cm^3 $molecule^{-1}s^{-1}$, for the H- and D-abstraction channels are, respectively, 4.11×10^{-19} and 5.01×10^{-20}, where the tunneling contributions are 5.31 and 3.38, respectively.

Quasi-classical trajectory (QCT) calculations[16−18] were carried out using the VENUS96 code,[19] customized to incorporate our analytical PES. Moreover, two modifications were included to compute the average energy in each normal mode to obtain information first on the temporal evolution of this energy along the first steps of the reaction, which is related to the quantum mechanical intramolecular vibrational redistribution (IVR) in the entry channel, and second on the CD_3 and CHD_2 coproducts vibrational distribution depending on the exit channel. In these modifications, the total energy in each normal mode is obtained as the sum of the kinetic and potential energies in each normal mode, *i*. The kinetic energy is obtained from the momentum matrix, P_R, and the reduced mass, μ,

$$(Ec)_i = \frac{1}{2\mu}(P_R)_i^2 \tag{1}$$

and the potential energy is obtained from the displacement matrix,

$$(Ep)_i = \frac{1}{2}\bar{\omega}_i(Q_R - Q_o)_i^2 \tag{2}$$

where Q_R and Q_o are the optimized geometries in Cartesian coordinates for the products and reactants, respectively, and $\bar{\omega}_i$ is the eigenvalue of mode *i*. This calculation is performed for each trajectory, and the total energy is then averaged. However, because VENUS freely rotates the molecules along the trajectories, the normal mode energy calculation is preceded by a rotation of the molecule to maintain the orientation of the optimized geometry of the respective products depending on the channel for which the normal-mode analysis was performed. Once this is done, a projection of the displacement and momentum matrices on the respective normal-mode space allows one to compute the potential and kinetic energies and, therefore, the total energy for each normal mode.

To study the IVR in CHD_3 (note that although our calculations are classical in nature, we use this nomenclature for clarity) we performed batches of 500 nonreactive trajectories. The initial conditions were set so that we ensured that no reaction takes place during the trajectory. Each set of trajectories was run for the CHD_3 ground-state and with a C−H stretch excitation by one quantum, and the energy for each normal mode was averaged for all trajectories in each case. The variation in each normal mode's average energy was taken as an indication of the internal flow of energy between normal modes in CHD_3. Note that this energy flow occurs before the collision with the H atom, so that it is not related to the mode−mode coupling along the reaction path (Coriolis-like terms) that we take as a qualitative indication of the energy flow when a reactive collision occurs.

To study the vibrational state of the CD_3 and CHD_2 products, the energy in each harmonic normal mode was computed for the last geometry (coordinates and momenta) on the reactive trajectories, and averaged for all the reactive trajectories. Because the harmonic approximation was used for this calculation, one could expect a breakdown of the procedure for highly excited states. However, as we are interested in the lowest CD_3 and CHD_2 vibrational states, we can assume that this method is accurate enough for the present purpose. This approach had been used in earlier papers by our group[14,20,21] with excellent results.

The accuracy of the trajectory was checked by the conservation of total energy and total angular momentum. The integration step was 0.01 fs, with an initial separation between the H atom and the CHD_3 molecule center of mass of 6.0 Å, and a rotational energy of 300 K. The maximum value of the impact parameter, b_{max}= 2.2 Å, was computed by calculating batches of 10 000 trajectories at fixed values of the impact parameter, *b*, system-

atically increasing the value of b until no reactive trajectories were obtained. To simulate the experimental conditions,[7] we considered a relative translational energy of 1.53 eV. To compare experimental and theoretical QCT results, for each reaction considered in this work, namely, CHD_3 ground-state and C−H stretch mode vibrationally excited, batches of 100.000 trajectories were calculated, where the impact parameter, b, was sampled by $b = b_{max}\, R^{1/2}$, with R being a random number in the interval [0,1].

A serious drawback of the QCT calculations is related to the question of how to handle the quantum mechanical zero-point energy (ZPE) problem in the classical mechanics simulation.[22−31] Many strategies have been proposed to correct for this quantum-dynamics effect (see, for instance, refs 22−26 and 29 and references therein), but no completely satisfactory alternatives have emerged. Here, we employed a pragmatic solution, the so-called passive method,[26] consisting of discarding all the reactive trajectories that lead, depending on the channel, to either an H_2 (HD) or a CD_3 (CHD_2) product with a vibrational energy below their respective ZPE. This we call histogram binning with double ZPE correction (HB-DZPE).

Finally, the mode−mode coupling along the reaction path (Coriolis-like terms) was analyzed using the Hamiltonian reaction path.[32] The kinetic energy is given by,

$$T(s,p_s,\{Q_m(s)\},\{P_m(s)\}) = \frac{1}{2\mu}\sum_{m}^{3N-7} P_m^2(s) + \frac{1}{2\mu}\frac{[p_s - \sum_{m=1}^{3N-7}\sum_{m'=1}^{3N-7} Q_m(s)P_{m'}(s)B_{mm'}(s)]^2}{[1 + \sum_{m=1}^{3N-7} Q_m(s)B_{mF}(s)]^2} \quad (3)$$

where p_s and $P_m(s)$ are the momenta conjugate to the reaction coordinate s and the $3N-7$ orthogonal normal-mode coordinates $Q_m(s)$, respectively. In this expression, $B_{mF}(s)$ and $B_{mm'}(s)$ are the so-called coupling terms along the reaction coordinate. The first, $B_{mF}(s)$, is the term measuring the coupling between the normal mode m and the motion along the reaction coordinate, F,

$$B_{m,F}(s) = -\sum_{i=1}^{N} \frac{d\nu_i(s)}{ds} \cdot L_{i,m}(s) \quad (4)$$

where $\nu_i(s)$ is component i of the normalized gradient vector, and $L_{i,m}(s)$ is component i of the eigenvector for mode m. These terms are the components of the reaction path curvature, $\kappa(s)$, defined as,

$$\kappa(s) = (\sum [B_{m,F}(s)]^2)^{1/2} \quad (5)$$

and they control the nonadiabatic flow of energy between these modes and the reaction coordinate.[33] The interest in the calculation of these coupling terms lies in the qualitative explanation of the possible vibrational excitation of reactants and products.

The $B_{mm'}(s)$ terms are the Coriolis-like coupling terms between modes, given by,

$$B_{m,m'}(s) = \sum_{i=1}^{N} \frac{dL_m(s)}{ds} L_{m'}(s) \quad (6)$$

and they give information about the energy flow between the vibrational modes in the reaction process.

3. Results and Discussion

3.1. Nomenclature and Coupling of the Normal Modes. To clarify the nomenclature used in the text, we shall start by describing the vibration normal modes in reactants (CHD_3) and products (H_2 and CD_3 for the first channel, and HD and CHD_2 for the second) obtained with the PES-2002 surface. The CHD_3 normal modes are: C−H stretch (ν_1, 3018 cm^{-1}), C−D asymmetric stretch (ν_4, 2260 cm^{-1}, doubly degenerate), C−D symmetric stretch (ν_2, 2090 cm^{-1}), rock bending (ν_5, 1282 cm^{-1}, doubly degenerate), deformation bending (ν_6, 1036 cm^{-1}, doubly degenerate), and umbrella bending (ν_3, 1021 cm^{-1}). The CD_3 free radical product normal modes are: C−D asymmetric stretch (ν_3, 2375 cm^{-1}, doubly degenerate), C−D symmetric stretch (ν_1, 2130 cm^{-1}), deformation bending (ν_4, 1016 cm^{-1}, doubly degenerate), and umbrella bending (ν_2, 449 cm^{-1}). The CHD_2 free radical product values are: C−H stretch (ν_1, 3133 cm^{-1}), C−D asymmetric stretch (ν_5, 2376 cm^{-1}), C−D symmetric stretch (ν_2, 2202 cm^{-1}), C−H bend (ν_6, 1266 cm^{-1}), scissors (ν_3, 1022 cm^{-1}), and out-of-plane bending (ν_4, 497 cm^{-1}). The H_2 and HD product stretching modes are 4406 and 3816 cm^{-1}, respectively.

For the first channel, we find that the C−H stretch mode, ν_1, is coupled to the reaction coordinate and evolves adiabatically to the H_2 stretching mode, while the CHD_3 umbrella bending mode, ν_3, evolves adiabatically to the CD_3 product umbrella mode, ν_2. For the second channel, the C−D symmetric stretch mode, ν_2, is coupled to the reaction coordinate and evolves adiabatically to the HD stretching mode, while the CHD_3 umbrella bending mode, ν_3, evolves adiabatically to the CHD_2 product out-of-plane mode, ν_4.

However, in previous work of our group,[11,34,35] we had found that this simple adiabatic model is incomplete and that coupling between the normal modes is significant, especially in the reactant valley, allowing some energy flow between the normal modes, and leading to a non-adiabatic picture. Following this idea, we also performed an exhaustive analysis of the vibrational mode coupling for the title reaction, H + CHD_3, using two approaches: first, by calculating the temporal evolution of the energy available in different vibrational modes (equivalent to quantum mechanical IVR) using QCT calculations, and second, by calculating the coupling terms between vibrational modes, $B_{mm'}$ (Coriolis-like terms).[32] The first approach can give some information about the energy flow among vibrational modes that takes place in the CHD_3 reactant preceding its collision with the H atom. The second approach gives information on the energy flow among the vibrational modes in the complex formed after the collision between the two reactants. This complex will eventually evolve into the activated complex and then reach the products.

Figure 1 shows the temporal evolution of the energy available in different vibrational modes for the ground-state CHD_3 reactant (Figure 1a) and after C−H stretch mode has been excited by one quantum (Figure 1b) averaged over all nonreactive trajectories. In both the CHD_3 ground-state and C−H stretch mode excited our classical trajectory calculations show a flux of energy from the C−D symmetric stretch, ν_2 mode, to the doubly degenerate rock bending, ν_5 mode, although quantum-mechanically the energy transferred does not suffice to excite the ν_5 mode, and the molecule remains in its ground-state. The effect of the C−H stretch excitation by one quantum (Figure 1b) is mostly to shift its corresponding curve to a higher energy, and

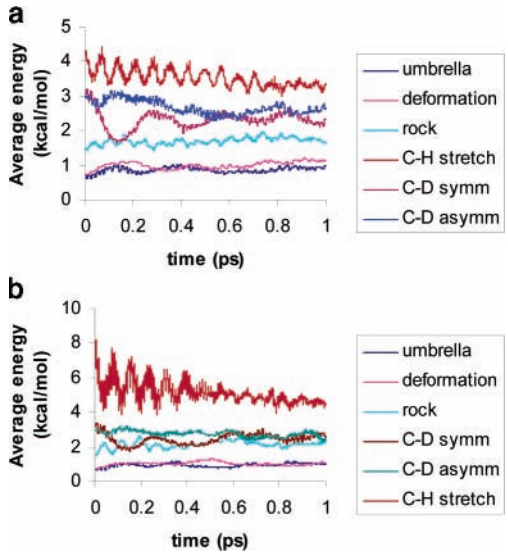

Figure 1. Average energy of each normal mode of CHD_3 from QCT calculations as a function of time. (a) Results for ground-state CHD_3. (b) Results for excitation of the C−H stretching mode by one quantum. The degenerate modes are represented by only one curve.

this mode will remain excited until CHD_3 collides with the H atom. Therefore, no transfer of energy is observed in the first steps for this reaction, and we conclude that the intramolecular vibrational redistribution will be small or negligible, in accordance with the Camden et al.'s suggestion based on experiment.[7]

Once the reactive collision occurs, the energy flow between modes can be monitored by the coupling terms $B_{mm'}$. Figure 2 shows the coupling matrix for the nine vibrational modes in CHD_3 along the reaction path for channels 1 and 2. In these plots the peaks indicate large coupling between the modes listed on the axes. In the first channel(Figure 2a), this coupling is especially important between the C−H stretching mode (ν_1) and the C−D symmetric (ν_2), $B_{mm'} = 38$ au, and asymmetric (ν_4), $B_{mm'} = 5$ au, stretch modes. In the second channel(Figure 2b), the situation is more complex. The coupling is especially important between the C−D symmetric stretch modes, ν_2, and the rock bending mode (ν_5); between the rock bending mode, ν_5, and the deformation bending mode (ν_6); and between the deformation bending mode (ν_6) and the umbrella mode, ν_3. All these coupling terms show values $B_{mm'} \approx 2$ au, and therefore smaller than the correspondent coupling terms for the channel 1. Therefore, there is significant mode mixing, and the reaction does not preserve vibrational adiabaticity along the reaction path, i.e., the reaction is nonadiabatic.

3.2. Product Energy Partition. The QCT results for the ground-state and C−H vibrationally excited $CHD_3(\nu)$ reactant at a collision energy of 1.53 eV are listed in Table 1 for the two channels, *P*1: $CD_3 + H_2$, and *P*2: $CHD_2 + HD$. Unfortunately, there is no experimental data for comparison, but we observe that when the C−H stretch mode is excited by one quantum the vibrational excitation of the CHD_2 product (channel 2) increases by a factor 2−3 with respect to the ground-state. This behavior agrees qualitatively with the experimental results of Camden et al.,[7] indicating that the C−H stretch mode preserves its character along the reaction. We shall return to this point below.

3.3. Product Vibrational Distribution. Table 2 lists the percentage vibrational distributions of the polyatomic product, CD_3 or CHD_2, depending on the channel *P*1 or *P*2, at a collision energy of 1.53 eV, where all the vibrational states of the diatomic product, H_2 or HD, respectively, are considered.

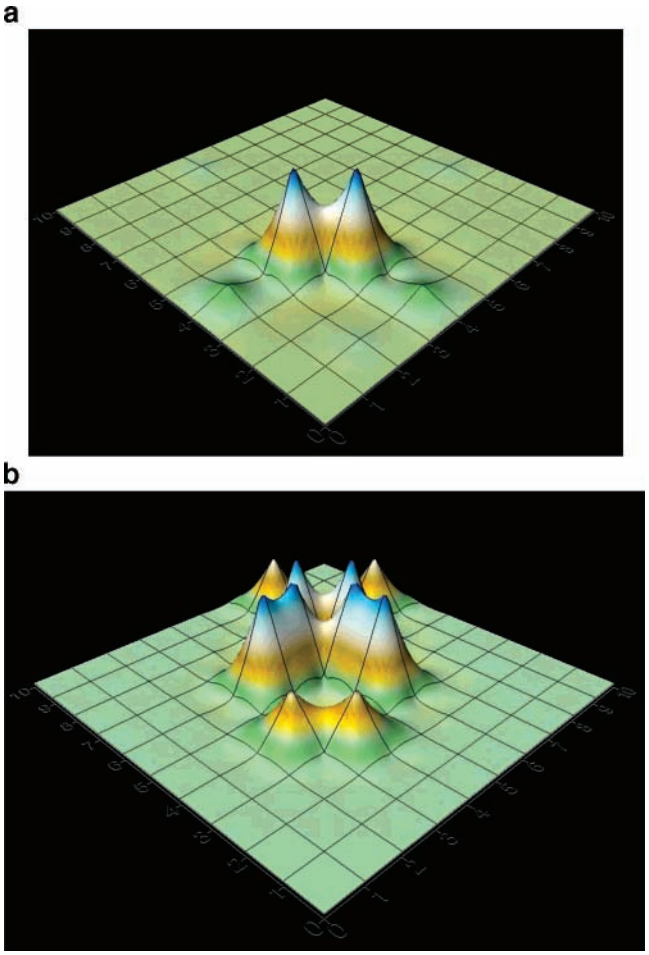

Figure 2. Coriolis-like $B_{mm'}$ coupling terms along the reaction path for the nine normal modes in CHD_3. The normal modes are numbered from higher to lower vibrational frequencies. Thus, mode 1 corresponds to ν_1, modes 2 and 3 correspond to ν_4, mode 4 to ν_2, 5 and 6 to ν_5, 7 and 8 to ν_6, and 9 to ν_3. (a) Coupling terms for channel 1, $CD_3 + H_2$; (b)values computed for channel 2, CHD_2 + HD. Note that a different scale was used in each Panel. So, the maximum value in (a) is 38, whereas in (b) it is 2.

TABLE 1: Product Energy Partition (in Percentages)[a] at a Collision Energy of 1.53 eV for the Two Channels, *P*1: $CD_3 + H_2$ and *P*2: CHD_2 + HD

	$CHD_3(\nu = 0)$		$CHD_3(\nu_1 = 1)$	
	*P*1	*P*2	*P*1	*P*2
$f_V(CD_3 \text{or} CHD_2)$[b]	11	8	7	20
$f_R(CD_3 \text{or } CHD_2)$	4	4	3	3
$f_V(H_2 \text{ or HD})$	16	20	15	17
$f_R(H_2 \text{or HD})$	8	6	10	6
f_T	61	62	65	54

[a] Calculated maximum error ±1. [b] Values of the products depending on the channel. f_V, f_R, and f_T mean vibrational, rotational, and translational contributions, respectively.

We begin by analyzing channel 1, $CD_3(\nu) + H_2$. The ground-state vibrational $CHD_3(\nu = 0)$ reactant gives mainly ground-state $CD_3(\nu = 0)$ products. The percentage diminishes with the modes: 25% with excited umbrella bending (ν_2), 9% with excited deformation bending (ν_4), and 0% in stretching excited modes. When the C−H stretch mode in CHD_3 is excited by one quantum, $\nu_1 = 1$, we find a similar CD_3 vibrational distribution, with the CD_3 product mainly in its ground-state.

TABLE 2: Percentage Population of CD_3 and CHD_2 Product Vibrational States at a Collision Energy of 1.53 eV

*P*1 channel, CD_3 product

	ν_2					ν_4			ν_1		ν_3	
	0	1	2	3	4	0	1	2	0	1	0	1
$CHD_3(\nu = 0)$	75	13	12	0	0	91	7	2	100	0	100	0
$CHD_3(\nu_1 = 1)$	83	11	4	1	1	95	5	0	100	0	100	0

*P*2 channel, CHD_2 product

	ν_4			ν_3			ν_6			ν_2			ν_5			ν_1		
	0	1	2	0	1	2	0	1	2	0	1	2	0	1	2	0	1	2
$CHD_3(\nu = 0)$	34	25	41	77	17	6	85	13	2	97	3	0	100	0	0	100	0	0
$CHD_3(\nu_1 = 1)$	53	24	23	90	8	2	93	7	0	98	2	0	98	2	0	12	77	11

TABLE 3: Reaction Cross-Section, σ_R (Å^2), at a Collision Energy of 1.53 eV

	This work		Xie-Bowman[a]	
CHD_3	*P*1[b]	*P*2[b]	*P*1	*P*2
$\nu_1 = 0$	0.08	0.16	0.04	0.08
$\nu_1 = 1$	0.26	0.37	0.49	0.10
$\nu_1 = 1/\nu_1 = 0$	3.2	2.3	12.2	1.2

[a] From ref 8. [b] *P*1 channel: $CD_3 + H_2$; *P*2 channel: $CHD_2 + HD$.

TABLE 4: State-to-State Reaction Cross-Section, σ_R (Å^2), at a Collision Energy of 1.53 eV

reactant state	products states	σ_R (Å^2)	percentage[a]
	$CHD_3(\nu_1 = 0)$ reactant ground-state		
$CHD_3(\nu_1 = 0)$	$CD_3(\nu_2 = 0) + H_2(\nu = 0)$	0.053	66
	$CD_3(\nu_2 = 0) + H_2(\nu = 1)$	0.006	8
	$CD_3(\nu_2 = 1,2) + H_2(\nu = 0)$	0.013	16
$CHD_3(\nu_1 = 0)$	$CHD_2(\nu_4 = 0) + HD(\nu = 0)$	0.041	25
	$CHD_2(\nu_4 = 0) + HD(\nu = 1)$	0.013	8
	$CHD_2(\nu_4 = 1,2) + HD(\nu = 0)$	0.056	35
	$CHD_2(\nu_4 = 1,2) + HD(\nu = 1)$	0.016	10
	$CHD_3(\nu_1 = 1)$ reactant C−H stretch mode excitation		
$CHD_3(\nu_1 = 1)$	$CD_3(\nu_2 = 0) + H_2(\nu = 0)$	0.175	67
	$CD_3(\nu_2 = 1,2) + H_2(\nu = 0)$	0.036	13
$CHD_3(\nu_1$=1)	$CHD_2(\nu_4 = 0) + HD(\nu = 0)$	0.144	39
	$CHD_2(\nu_4 = 1,2) + HD(\nu = 0)$	0.098	26
	$CHD_2(\nu_4 = 1,2) + HD(\nu = 1)$	0.030	8
$CHD_3(\nu_1 = 1)$	$CHD_2(\nu_1 = 0) + HD(\nu = 0)$	0.031	8
	$CHD_2(\nu_1 = 1) + HD(\nu = 0)$	0.213	57
	$CHD_2(\nu_1 = 1) + HD(\nu = 1)$	0.067	18
	$CHD_2(\nu_1 = 2) + HD(\nu = 0)$	0.029	8

[a] Percentage of the total reaction cross-section for each channel. The differences from 100 in each channel correspond to minor paths (<8%). In the last reaction, $CHD_3(\nu_1 = 1) + H$, channel 2, we have separated the contributions for each CHD_2 vibrational state, ν_4 and ν_1, to avoid double counting the HD contributions.

These theoretical results agree with the experimental evidence,[7] indicating that the reactant vibrational excitation has a little influence on the CD_3 product state distribution for channel 1. Next, we shall analyze channel 2, $CHD_2(\nu) + HD$. In general, the $CHD_2(\nu)$ vibrational distribution is broader than in the earlier case, $CD_3(\nu)$, and the ground-state vibrational $CHD_3(\nu)$ reactant gives CHD_2 products that are more excited, 66% in the ν_4 mode, 23% in the ν_3 mode, or 15% in the ν_6 mode. The three stretching modes appear practically in the ground-state. The excitation of the C−H stretch mode by one quantum, $\nu_1 = 1$, changes the situation sharply. The ν_4, ν_3, and ν_6 modes are still excited, but now the C−H stretch mode in CHD_2, mode ν_1, appears vibrationally excited, 77%. These theoretical results reproduce the experimental information[7] indicating that the C−H stretch mode excitation is maintained along the reaction, i.e., the reaction presents mode selectivity.

3.4. Reaction Cross-Section. The QCT reaction cross-sections, σ_R, at a collision energy of 1.53 eV, for the two channels *P*1 and *P*2 are listed in Table 3, together with other theoretical values[8] for comparison.

For the ground-state reaction, $CHD_3(\nu_1 = 0)$, it was found experimentally that the H- or D-abstractions show no clear preference, and due to experimental difficulties with the isotopic substitution a quantitative ratio was not reported. The cross-section ratio, *P*2/*P*1, ($CHD_2 + HD/CD_3 + H_2$), obtained in the present study, is 2, i.e., the D-abstraction is favored, which agrees with experiment, and quantitatively with the QCT results by Xie and Bowman[8] on a very different surface. Statistically, one would expect a ratio 3:1 (D versus H), but the 2:1 ratio found can be explained because the maximum of the vibrationally adiabatic curve for the D-abstraction is 0.95 kcal mol^{-1} higher than for the H-abstraction.

When the C−H stretch mode in $CHD_3(\nu_1 = 1)$ is excited by one quantum, unfortunately the experimental measurements[7] only report a qualitative description, in particular that for both two channels, $CD_3(\nu = 0) + H_2$ and $CHD_2(\nu_1 = 1) + HD$, the excitation of the C−H stretch mode increases the reactivity with respect to the reactant ground-state. These results suggest that the simple spectator model is not enough to explain this behavior. Thus, the vibrational excitation localized in the C−H stretch mode is also able to enhance the reactivity of the D-abstraction. Our QCT results reproduce this behavior, and qualitatively agree with other QCT results[8] on a different PES, although those authors report a greater value for channel 1. The reaction cross-section ratio found in the present study for the $H + CHD_3(\nu_1 = 0,1)$ reaction due to the C−H stretch mode excitation, 3.2 and 2.3, for channels 1 and 2, respectively, agrees with recent QCT results from our group[14] for the similar $H + CH_4(\nu_1 = 0,1)$ reaction, where a factor of about 2 is reported, which agrees with experimental values,[3] 3.0 ± 1.5.

Experimentally, Camden et al.[7] focused their study on the detection of the polyatomic products, CD_3 or CHD_2, depending on the channel, ignoring the diatomic product state, H_2 or HD, respectively. In the present study, for the first time for this reaction, we have performed a theoretical state-to-state study. Because of the large number of paths opened for the title reaction, especially when vibrational excitations are considered, we focused the study on those paths with a participation ≥8% of the total reactivity. Table 4 lists the state-to-state reaction cross-section for $CHD_3(\nu_1 = 0,1)$ at a collision energy of 1.53 eV. First, as was anticipated in Section 3.3, the vibrational spectra for channel 2, $CHD_2(\nu) + HD(\nu)$, is more complex than that of the channel 1, $CD_3(\nu) + H_2(\nu)$. For channel 2 the number of product paths is greater than for channel 1, especially when the C−H stretch excitation is considered. Second, for channel

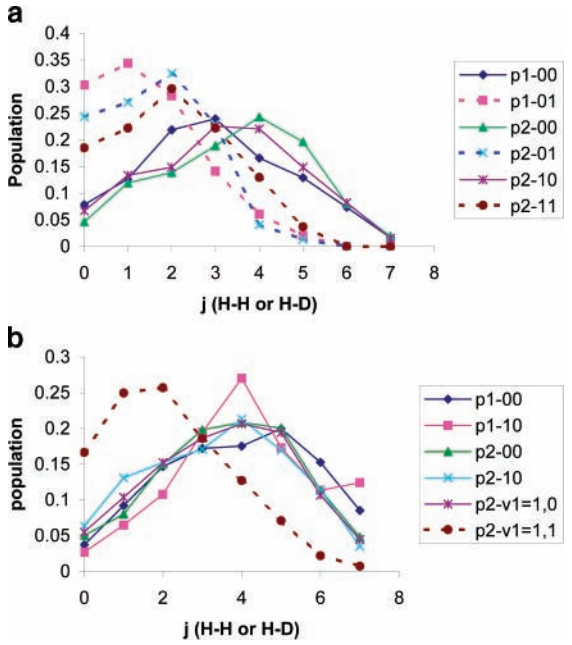

Figure 3. Rotational populations for H + CHD_3 reaction at a collision energy of 1.53 eV. The distributions are normalized so that the area under the common levels is the same. *P*1, H-abstraction, channel 1, leads to the CD_3 + H_2 products; *P*2, D-abstraction, channel 2, leads to the CHD_2 + HD products. The number after *P*1 or *P*2 corresponds to the vibrational state of the polyatomic and diatomic products, respectively. For instance, *P*1−00 corresponds to channel 1 with the CD_3 and H_2 in their respective ground-states. The notation *P*2 − v1 = 1,0 corresponds to channel 2 with the CHD_2 excited by one quantum in the C−H stretch and the HD in its ground-state. (a) and (b) Reactant $CHD_3(\nu)$ ground-state and C−H stretch mode excitation, respectively.

1 the main reactions lead to CD_3 and H_2 products in their respective ground-states, for the CHD_3 reactant both in its ground-state and vibrationally excited: 66 and 67%, respectively,

$$H + CHD_3(\nu_1 = 0,1) \rightarrow CD_3(\nu = 0) + H_2(\nu = 0)$$

Channel 2 leads mainly also to CHD_2 and HD products in their ground-states, although now the contribution of the excitation of the out-of-plane mode, ν_4, is important, and this behavior is similar for the CHD_3 reactant in its ground and vibrationally excited states. Moreover, for this channel the contribution of the vibrationally excited C−H stretch mode in the product, $CHD_2(\nu_1 = 1)$, is important for the vibrationally excited CHD_3 reactant, being 57% of the total reactivity,

$$H + CHD_3(\nu_1 = 0,1) \rightarrow CHD_2(\nu_4 = 0,1,2) + HD(\nu = 0)$$
$$\rightarrow CHD_2(\nu_1 = 1) + HD(\nu = 0)$$

Third, unfortunately there are neither experimental nor theoretical data for comparison, so that the present theoretical calculations are predictive, to be confirmed (or not) in future experiments.

3.5. Rotational Distributions of the Bimolecular Products, H_2 and HD. The rotational distributions of the H_2 and HD products at a collision energy of 1.53 eV for the main state-to-state paths are plotted in Figure 3 for the CHD_3 reactant in its ground-state (Figure 3a) and C−H stretch mode excitation (Figure 3b).

In general, for the main state-to-state paths the bimolecular products in their vibrational ground-states, $H_2(\nu = 0)$ and $HD(\nu = 0)$ appear hotter, $j = 3-4$, and the distributions are

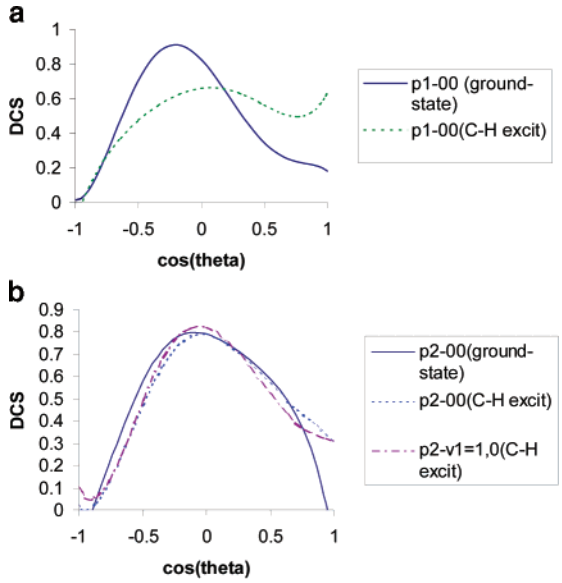

Figure 4. Product angular distribution for the H + CHD_3 reaction at a collision energy of 1.53 eV, for the main paths in both channels. The distributions are normalized so that the area under the common levels is the same. (a) Channel 1, *P*1, with the CHD_3 reactant in its ground-state and with the C−H stretch mode excited. (b) Channel 2, *P*2, with the CHD_3 reactant in its ground-state and with the C−H stretch mode excited.

broader, than in their vibrationally excited states, $H_2(\nu = 1)$ and $HD(\nu = 1)$, $j = 1-2$, which is the expected behavior. This tendency is independent of whether or not the CHD_3 reactant is vibrationally excited. Unfortunately, there are no experimental values for comparison, and the only available theoretical results[8] do not differentiate state-to-state.

3.6. Scattering Distributions of the Polyatomic Products, CD_3 and CHD_2. It is well-known that one of the main limitations of the traditional histogram binning procedure used in the QCT calculations is that it gives product rotational distributions hotter and broader than experimental measurements. In atom + diatom systems this seems to be a general tendency, and moreover when the dimensionality of the system increases, the distributions seem to have an artificial tail extending to very high rotational levels.[36−40] In an earlier study on the Cl + CH_4 reaction,[41] we observed that the product rotational distribution obtained with QCT calculations greatly influences the angular scattering distribution, and only when the lowest rotational numbers are considered is the experimental measurement reproduced. Therefore, in the present study, we assume this behavior, and the product scattering distribution (measured as the differential cross section, DCS) is analyzed using only trajectories with the lowest *j* values, between 0 and 2.

The angular scattering distributions at a collision energy of 1.53 eV for the main state-to-state paths, considering the CHD_3 reactant in both its ground and vibrationally excited states, are plotted in Figure 4 for channel 1, CD_3 + H_2 (Figure 4a) and channel 2, CHD_2 + HD (Figure 4b). For the CHD_3 reactant in its ground-state, both channels yield predominantly sideways scattered CD_3 and CHD_2, respectively. When the C−H stretch mode is excited by one quantum, these distributions are more forward, suggesting an increased contribution of the rebound mechanism associated with low impact parameters.

Unfortunately, there is no experimental information on the title reaction for comparison. However, for the similar H + CD_4 → CD_3 + HD ground-state reaction, Zare and co-workers[42−44] find that the CD_3 products are sideways/backward scattered,

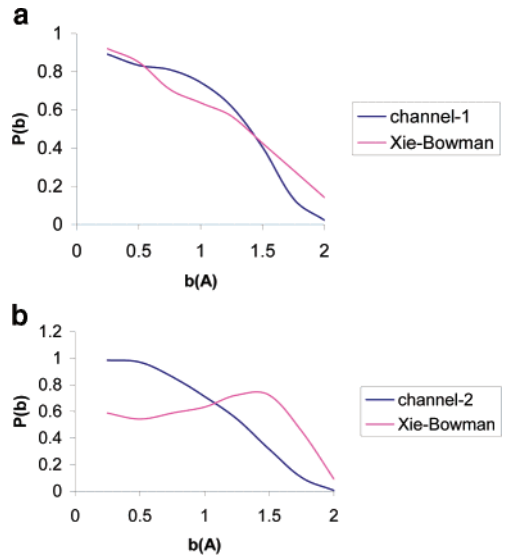

Figure 5. Opacity function (reaction probability, $P(b)$, versus impact parameter, b) for channel 1 (a) and 2 (b), with the CHD_3 reactant in its ground-state, together with the Xie and Bowman's results for comparison.[8] In each Panel, the distributions are normalized so that the area under the common levels is the same.

$<\cos\theta> = -0.20 \pm 0.09$ at 1.95 eV, and $<\cos\theta> = -0.07 \pm 0.10$ at 1.2 eV. For the CHD_3 reactant ground-state at 1.53 eV we obtain $<\cos\theta> = -0.05$ for channel 1, and $<\cos\theta> = +0.03$ for channel 2. The C−H stretch excitation of the CHD_3 reactant produces a shift toward forward angles, $<\cos\theta> = +0.13$ and $+0.11$ for channels 1 and 2, respectively.

Xie and Bowman's QCT calculations[8] yield a similar picture for channel 2, for the CHD_3 reactant both in its ground-state and in the excited state, but remarkably different for channel 1, especially for the CHD_3 in its ground-state, where those authors suggest a rebound mechanism. A direct comparison with the present QCT calculations is very difficult because several factors are involved. First, there is the influence of the diatomic molecule rotational distribution on the scattering distribution. As was observed previously,[41] larger values of j favor forward scattering. Whereas we obtain values of j up to 7, Xie and Bowman found larger values, up to 15. Second, there is the influence of the opacity function (reaction probability, $P(b)$, versus impact parameter, b) on the scattering distribution. It is known that the contribution of larger impact parameters leads to backward-scattered products. Figure 5 plots the opacity function for the CHD_3 ground-state in channel 1 (Figure 5a) and channel 2 (Figure 5b), together with the values of Xie and Bowman for comparison. While for the channel 1 both results are similar, for the channel 2 the values of Xie and Bowman are shifted to larger b values, favoring backward scattering. Therefore, it is observed that these two effects have contrary behavior. It is impossible to say at this time what the weight of each factor is, only that while in the present calculation the two effects compensate each other, in the Xie-Bowman's paper the contribution of the rotational number in channel 1 is not compensated with the opposite contribution from the opacity function. Moreover, to further complicate this direct comparison, two other factors are involved. First, whereas Xie and Bowman do not differentiate state-to state, in the present study a state-to-state calculation was performed. Second, the QCT calculations are performed with different code programs, VENUS96 in the present study, whereas Xie and Bowman used their own code.

4. Conclusions

In this paper we have performed exhaustive state-to-state QCT calculations with the aim of analyzing the effect of the C−H stretch mode excitation in CHD_3 on the dynamics of its reaction with a hydrogen atom, which can evolve along two channels, $CD_3 + H_2$, and $CHD_2 + HD$. A collision energy of 1.53 eV was considered for comparison with experiment and other QCT calculations. Before the collision between the reactants, no transfer of energy between vibrational modes is observed for this reaction, and once the reaction occurs strong coupling between some vibrational modes is found, allowing the non-adiabatic flow of energy between modes. Therefore, they do not preserve their adiabatic character along the reaction path, i.e., the reaction is non-adiabatic. This behavior has also been previously reported for the similar $H + CH_4$ reaction.

1. The C−H stretch mode excitation by one quantum increases the reactivity with respect to the vibrational ground-state by factors ∼3 and ∼2 for the H-abstraction, $CD_3 + H_2$, and D-abstraction, $CHD_2 + HD$, respectively. These results agree with the experimental evidence.

2. For channel 1, $CD_3 + H_2$, the C−H stretch mode excitation has little influence on the product rovibrational distributions. For channel 2, $CHD_2 + HD$, whereas the C−H excitation has little influence on the HD rotational distribution, it increases the C−H stretch mode excitation in the CHD_2 product, indicating that the reaction shows mode selectivity. These rovibrational results also agree with experiment.

3. For the CHD_3 reactant in its vibrational ground-state, the $CD_3 + H_2$ and $CHD_2 + HD$ channels yield predominantly sideways scattered CD_3, $<\cos\theta> = -0.05$, and CHD_2, $<\cos\theta> = +0.03$, respectively. The C−H stretch mode excitation by one quantum leads to a shift toward forward scattering for both channels. These results qualitatively agree with those by Xie and Bowman, except for the channel 1 with the CHD_3 ground state. Finally, these theoretical results are predictive, because unfortunately there is no experimental information for comparison.

Acknowledgment. This work was partially supported by the Junta de Extremadura, Spain (Project No. 2PR04A001).

References and Notes

(1) Bechtel, H. A.; Camden, J. P.; Brown, D. J. A.; Zare, R. N. *J. Chem. Phys.* **2004**, *120*, 5096.
(2) Kim, Z. H.; Bechtel, H. A.; Camden, J. P.; Zare, R. N. *J. Chem. Phys.* **2005**, *122*, 084303.
(3) Camden, J. P.; Bechtel, H. A.; Brown, D. J. A.; Zare, R. N. *J. Chem. Phys.* **2005**, *123*, 134301.
(4) Yoon, S.; Henton, S.; Zirkovic, A. N.; Crim, F. F. *J. Chem. Phys.* **2002**, *116*, 10744.
(5) Yoon, S.; Holiday, R. J.; Crim, F. F. *J. Chem. Phys.* **2003**, *119*, 4755.
(6) Yoon, S.; Holiday, R. J.; Silbert, E. L., III.; Crim, F. F. *J. Chem. Phys.* **2003**, *119*, 9568.
(7) Camden, J. P.; Bechtekl, H. A.; Brown, D. J. A.; Zare, R. N. *J. Chem. Phys.* **2006**, *124*, 034311.
(8) Xie, Z.; Bowman, J. M. *Chem. Phys. Lett.* **2006**, *429*, 355.
(9) Zhang, X.; Braams, B. J.; Bowman, J. M. *J. Chem. Phys.* **2006**, *124*, 021104.
(10) Xie, Z.; Bowman, J. M.; Zhang, X. *J. Chem. Phys.* **2006**, *125*, 133120.
(11) Espinosa-García, J. *J. Chem. Phys.* **2002**, *116*, 10664.
(12) Rangel, C.; García-Bernáldez, J.; Espinosa-García, J. *Chem. Phys. Lett.* **2006**, *422*, 581.
(13) Rangel, C.; Sansón, J.; Corchado, J. C.; Espinosa-García, J.; Nyman, G. *J. Phys. Chem. A* **2006**, *110*, 10715.
(14) Rangel, C.; Corchado, J. C.; Espinosa-García, J. *J. Phys. Chem. A* **2006**, *110*, 10375.
(15) Zhao, Y.; Yamamoto, T.; Miller, W. H. *J. Chem. Phys.* **2004**, *120*, 3100.

(16) Porter, R. N.; Raff, L. M. In *Dynamics of Molecular Collisions*, part B; Miller, W. H., Ed.; Plenum Press: New York, 1976.
(17) Truhlar, D. G.; Muckerman, J. T. In *Atom-Molecules Collision Theory*; Bernstein, R. B., Ed.; Plenum Press: New York, 1979.
(18) Raff, L. M.; Thompson, D. L. In *Theory of Chemical Reaction Dynamics*; Baer, M., Ed.; CRC Press: Boca Raton, FL, 1985; Vol. 3.
(19) Hase, W. L.; Duchovic, R. J.; Hu, X.; Komornicki, A.; Lim, K. F.; Lu, D-h.; Peslherbe, G. H.; Swamy, K. N.; Van de Linde, S. R.; Varandas, A. J. C.; Wang, H.; Wolf, R. J. VENUS96: A General Chemical Dynamics Computer Program. *QCPE Bull.* **1996**, *16*, 43.
(20) Espinosa-García, J.; Bravo, J. L.; Rangel, C. *J. Phys. Chem. A* **2007**, *111*, 2761.
(21) Espinosa-García, J. *J. Phys. Chem. A* **2007**, *111*, 3497.
(22) Bowman, J. M.; Kuppermann, A. *J. Chem. Phys*. **1973**, *59*, 6524.
(23) Truhlar, D. G. *J. Phys. Chem*. **1979**, *83*, 18.
(24) Schatz, G. C. *J. Chem. Phys*. **1983**, *79*, 5386.
(25) Lu, D-h.; Hase, W. L. *J. Chem. Phys*. **1988**, *89*, 6723.
(26) Varandas, A. J. C. *Chem. Phys. Lett.* **1994**, *225*, 18.
(27) Ben-Nun, M.; Levine, R. D. *J. Chem. Phys*. **1996**, *105*, 8136.
(28) McCormack, D. A.; Lim, K. F. *Phys. Chem. Chem. Phys*. **1999**, *1*, 1.
(29) Stock, G.; Müller, U. *J. Chem. Phys*. **1999**, *111*, 65.
(30) Marques, J. M. C.; Martinez-Nuñez, E.; Fernandez-Ramos, A.; Vazquez, S. *J. Phys. Chem.* **2005**, *109*, 5415.
(31) Duchovic, R. J.; Parker, M. A. *J. Phys. Chem*. **2005**, *109*, 5883.
(32) Miller, W. H.; Handy, N. C.; Adams, J. E. J. *Chem. Phys.* **1980**, *72*, 99.
(33) Kraka, E.; Dunning, T. H. In *Advances in Molecular Electronic Structure Theory*; JAI: New York, 1990; Vol. I, p 129.
(34) Sanson, J.; Corchado, J. C.; Rangel, C.; Espinosa-Garcia, J. *J. Chem. Phys.* **2006**, *124*, 074312.
(35) Sanson, J.; Corchado, J. C.; Rangel, C.; Espinosa-Garcia, J. *J. Phys. Chem. A* **2006**, *110*, 9568.
(36) Wang, X.; Ben-Nun, M.; Levine, R. D. *Chem. Phys*. **1995**, *197*, 1.
(37) Troya, D.; Millan, J.; Baños, I.; Gonzalez, M. *J. Chem. Phys*. **2002**, *117*, 5730.
(38) Troya, D. *J. Chem. Phys*. **2005**, *123*, 214305.
(39) Castillo, J. F.; Aoiz, F. J.; Bañares, L.; Martinez-Nuñez, A.; Fernández-Ramos, A.; Vazquez, S. *J. Phys. Chem*. A **2005**, *109*, 8459.
(40) Troya, D.; Weiss, P. J. E. *J. Chem. Phys*. **2006**, *124*, 074313.
(41) Rangel, C.; Navarrete, M.; Corchado, J. C.; Espinosa-García, J. *J. Chem. Phys.* **2006**, *124*, 124306.
(42) Camden, J. P.; Bechtel, H. A.; Zare, R. N. *Angew. Chem., Int. Ed.* **2003**, *42*, 5227.
(43) Camden, J. P.; Bechtel, H. A.; Brown, D. J. A.; Martin, M. R.; Zare, R. N.; Hu, W.; Lendvay, G.; Troya, D.; Schatz, G. C. *J. Am. Chem. Soc.* **2005**, *127*, 11898.
(44) Camden, J. P.; Hu, W.; Bechtel, H. A.; Brown, D. J. A.; Martin, M. R.; Zare, R. N.; Lendvay, G.; Troya, D.; Schatz, G. C. *J. Phys. Chem. A* **2006**, *110*, 677.